

Cherenkov phase matched THz-wave generation with surfing configuration for bulk Lithium Niobate crystal

Koji Suizu^{1,*}, Toshihiro Tsutsui¹, Takayuki Shibuya^{1,2}, Takuya Akiba¹, and Kodo Kawase^{2,3}

¹ Department of Electrical Engineering, Nagoya University, Furo-cho, Chikusa-ku, Nagoya 464-8603, Japan

² RIKEN, 519-1399 Aramaki-Aoba, Aoba, Sendai 980-0845, Japan

³ EcoTopia Science Institute, Nagoya University Furo-cho, Chikusa-ku, Nagoya 464-8603, Japan
suizu@nuee.nagoya-u.ac.jp

Abstract: We demonstrated a Cherenkov phase matched THz-wave generation with surfing configuration for bulk lithium niobate crystal. THz-wave output was enhanced about 50 times by suppressing phase mismatching for THz-wave propagation direction. The suppression was achieved by combining two pumping waves with dual wavelength with finite angle, and THz-frequency was controllable by changing the angle within 2.5 degrees range. Higher frequency THz-wave generation at around 4.0 THz was successfully obtained by the method.

©2009 Optical Society of America

OCIS codes: (190.4223) Nonlinear wave mixing; (190.4410) Nonlinear optics, parametric processes

References and links

1. G. D. Boyd, T. J. Bridges, C. K. N. Patel, and E. Buehler, "Phase-matched submillimeter wave generation by difference-frequency mixing in ZnGeP₂," *Appl. Phys. Lett.* **21**, 553–555 (1972).
2. A. Rice, Y. Jin, X. F. Ma, X. C. Zhang, D. Bliss, J. Larkin, and M. Alexander, "Terahertz optical rectification from <110> zinc-blende crystals," *Appl. Phys. Lett.* **64**, 1324–1326 (1994).
3. W. Shi, Y. J. Ding, N. Fernelius, and K. Vodopyanov, "Efficient, tunable, and coherent 0.18–5.27-THz source based on GaSe crystal," *Opt. Lett.* **27**, 1454–1456 (2002).
4. T. Tanabe, K. Suto, J. Nishizawa, K. Saito, and T. Kimura, "Tunable terahertz wave generation in the 3- to 7-THz region from GaP," *Appl. Phys. Lett.* **83**, 237–239 (2003).
5. Y. Avetisyan, Y. Sasaki, and H. Ito, "Analysis of THz-wave surface-emitted difference-frequency generation in periodically poled lithium niobate waveguide," *Appl. Phys. B* **73**, 511–514 (2001).
6. Y. Sasaki, Y. Avetisyan, K. Kawase, and H. Ito, "Terahertz-wave surface-emitted difference frequency generation in slant-stripe-type periodically poled LiNbO₃ crystal," *Appl. Phys. Lett.* **81**, 3323–3325 (2002).
7. Y. Sasaki, Y. Avetisyan, H. Yokoyama, and H. Ito, "Surface-emitted terahertz-wave difference frequency generation in two-dimensional periodically poled lithium niobate," *Opt. Lett.* **30**, 2927–2929 (2005).
8. Y. Sasaki, H. Yokoyama, and H. Ito, "Surface-emitted continuous-wave terahertz radiation using periodically poled lithium niobate," *Electron. Lett.* **41**, 712–713 (2005).
9. D. H. Auston, K. P. Cheung, J. A. Valdmanis, and D. A. Kleinman, "Cherenkov radiation from femtosecond optical pulses in electro-optic media," *Phys. Rev. Lett.* **53**, 1555–1558 (1984).
10. D. A. Kleinman and D. H. Auston, "Theory of electro-optic shock radiation in nonlinear optical media," *IEEE J. Quantum Electron.* **20**, 964–970 (1984).
11. J. Hebling, G. Almasi, I. Kozma, and J. Kuhl, "Velocity matching by pulse front tilting for large area THz-pulse generation," *Opt. Express* **10**, 1161–1166 (2002).
12. K.-L. Yeh, M. C. Hoffmann, J. Hebling, and K. A. Nelson, "Generation of 10 μJ ultrashort THz pulses by optical rectification," *Appl. Phys. Lett.* **90**, 171121 (2007).
13. S. B. Bodrov, A. N. Stepanov, M. I. Bakunov, B. V. Shishkin, I. E. Ilyakov, and R. A. Akhmedzhanov, "Highly efficient optical-to-terahertz conversion in a sandwich structure with LiNbO₃ core," *Opt. Express* **17**, 1871–1879 (2009).
14. K. Suizu, T. Tutui, T. Shibuya, T. Akiba, and K. Kawase, "Cherenkov phase-matched monochromatic THz-wave generation using difference frequency generation with lithium niobate crystal," *Opt. Express* **16**, 7493–7498 (2008).
15. H. Ito and T. Ikari et al. recently clarified that a pulse energy of about 101 pJ/pulse corresponded to a Si-bolometer voltage output of 1 V. We adopted the novel calibration data.
16. R. L. Sutherland, *Handbook of Nonlinear Optics*, (Marcel Dekker, New York (2003), Chap. 2.

17. T. Shibuya, T. Tsutsui, K. Suizu, T. Akiba, and K. Kawase, "Efficient Cherenkov-Type Phase-Matched Widely Tunable THz-Wave Generation via an Optimized Pump Beam Shape," *Appl. Phys. Express* **2**, 032302 (2009).
 18. J. K. Wahlstrand and R. Merlin, "Cherenkov radiation emitted by ultrafast laser pulses and the generation of coherent polaritons," *Phys. Rev. B* **68**, 054301 (2003).
 19. D. H. Jundt, "Temperature-dependent sellmeier equation for the index of refraction, n_e , in congruent lithium niobate," *Opt. Lett.* **22**, 1553-1555 (1997).
 20. H. Ito, K. Suizu, T. Yamashita, and T. Sato, "Random frequency accessible broad tunable terahertz-wave source using phase-matched 4-dimethylamino-N-methyl-4-stilbazolium tosylate (DAST) crystal," *Jpn. J. Appl. Phys.* **46**, 7321-7324 (2007).
 21. L. Palfalvi, J. Hebling, J. Kuhl, A. Peter, and K. Polgar, "Temperature dependence of the absorption and refraction of Mg-doped congruent and stoichiometric LiNbO₃ in the THz range," *J. Appl. Phys.* **97**, 123505 (2005).
 22. K. Suizu, T. Shibuya, S. Nagano, T. Akiba, K. Edamatsu, H. Ito, and K. Kawase, "Pulsed high peak power millimeter wave generation via difference frequency generation using periodically poled lithium niobate," *Jpn. J. Appl. Phys.* **46**, L982 - L984 (2007).
 23. K. Kawase, H. Minamide, K. Imai, J. Shikata, and H. Ito, "Injection-seeded terahertz-wave parametric generator with wide tunability," *Appl. Phys. Lett.* **80**, 195-197 (2002).
 24. P. E. Powers, R. A. Alkuwari, J. W. Haus, K. Suizu, H. Ito, "Terahertz generation with tandem seeded optical parametric generators," *Opt. Lett.* **30**, pp. 640-642 (2005).
-

1. Introduction

Terahertz (THz)-wave is very attractive spectral regions, for advanced applications, involving biomedical analysis, stand-off detection for hazardous materials, etc. The development of monochromatic and tunable coherent THz-wave sources is of great interest for use in these applications. Recently, a parametric process based on second-order nonlinearities has been used to generate tunable monochromatic coherent THz-waves using nonlinear optical (NLO) crystals [1-4]. In general, however, nonlinear optical materials have high absorption coefficients in the THz-wave region, which prevents efficient THz-wave generation.

Avetisyan et al. proposed surface-emitting THz-wave generation by difference frequency generation (DFG) in a periodically poled lithium niobate (PPLN) waveguide to overcome these problems [5]. A surface-emitted THz wave radiates from the surface of PPLN and propagates perpendicular to the direction of the pump beam. The absorption loss is minimized because the THz wave is generated from the PPLN surface [6-7]. Moreover, the phase-matching condition can be designed using PPLN with an appropriate grating period. Surface emitted THz-wave device has a potential for realizing high conversion efficiency, and continuous wave THz-wave generation was successfully demonstrated [8]. Unfortunately, tuning range of THz-wave is limited by design of PPLN, each PPLN has about 100 GHz of tuning range. Wide tuning range cannot be realized by quasi phase matching method.

We demonstrated Cherenkov phase matching method [9-13] for monochromatic THz-wave generation via DFG process using bulk lithium niobate crystal [14]. We successfully generated monochromatic THz-waves with wide tunability in the range 0.2–2.5 THz. The highest THz-wave energy was about 800 pJ/pulse [15], and this energy could be obtained for the broad spectral region in the range around 0.2–2.0 THz. Although we successfully got wide tunable characteristics of THz-wave generation, conversion efficiency of a THz-wave generation at higher frequency region above 2.0 THz was slightly low. It would be caused by phase mismatch of generated THz-wave in a propagating direction of THz-wave. Beam diameter of pumping waves in a lithium niobate crystal in our previous work was about 300 μm , which corresponded to about ten cycles of THz waves at 2.0 THz because the refractive index of lithium niobate is about 5.2 [16]. THz-wave generated at far from a crystal surface interfered with that generated at neighborhood of a crystal surface, resulted in denying each other. By reducing the width of beam diameter in the crystal in the direction of THz-wave propagation to about one-half of the THz wavelength, there was no need to consider phase matching in that direction. We observed the effects by condensing a pump beam diameter to a THz-wave propagation direction by cylindrical lenses [17]. Although higher THz-wave around 4.0 THz was successfully generated under tight focusing by the cylindrical lens with

20 mm of focus length, output of THz-wave at lower frequency region was reduced, because tight focusing resulted in reducing interaction length for pumping wave propagating direction

2. Cherenkov phase mating with surfing configuration

In this study, we propose surfing configuration of Cherenkov type phase matching for THz-wave generation for bulk crystal to suppress a phase mismatching. Interference pattern of pumping waves in the crystal is induced by combining the dual wavelengths beams with finite angle. It provides a same spatial pattern of second order nonlinear polarization in THz-frequency. The interference pattern has not checkerboard one, which is a results of interference of tilted beams with same frequency, like as mentioned in Ref. 18, because dual wavelength beam courses other spatial interference pattern, corresponding to difference frequency, and the interference pattern is superimposed in checkerboard one.

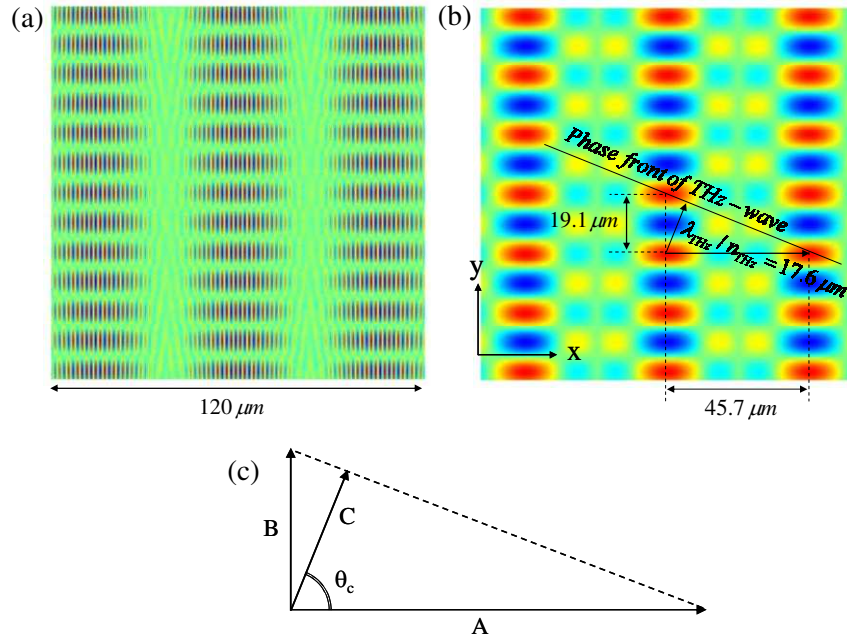


Fig. 1. Normalized electric field distribution of (a) combined dual wavelength pump beams with finite angle, and (b) exited second order nonlinear polarization of difference frequency. Here, $\lambda_1=1300$ nm, $\lambda_2=1317$ nm and 3 THz of difference frequency with 3.7 degrees of beam angle. (c) Geometric relation of A: excited nonlinear polarization for x-direction, B: interference period of pump beams for y-direction and C: THz-wavelength in the crystal.

Figure 1 shows electric field distribution of (a) pumping waves and (b) excited nonlinear polarization, with $\lambda_1=1300$ nm, $\lambda_2=1317$ nm (here, three waves in DFG interaction has a relation of $\omega_1=\omega_2-\omega_{\text{THz}}$, and corresponding THz frequency is 3 THz) and 3.7 degrees of angle between divided pumping beams, α . The periods of nonlinear polarization pattern of dual wavelengths beams, A for x-axis and B for y-axis are represented by following equations,

$$\begin{cases} A = \frac{2\pi}{(k_1 - k_2)\cos\frac{\alpha}{2}} \\ B = \frac{4\pi}{(k_1 + k_2)\sin\frac{\alpha}{2}} \end{cases} \quad (1)$$

where $k_1=2\pi n_1/\lambda_1$ and $k_2=2\pi n_2/\lambda_2$, here n_1 and n_2 are refractive index of λ_1 and λ_2 , respectively. We used Sellmeier equation at near-infrared region for a lithium niobate crystal from Ref. 19. On the other hands, Cherenkov angle of the crystal, θ_c , is decided by relation of length A and THz-wavelength in the crystal, $C=\lambda_{\text{THz}}/n_{\text{THz}}$, here λ_{THz} and n_{THz} are THz-wavelength in vacuum and refractive index of the crystal at THz frequency. A phase matching condition for THz-wave propagation direction is satisfied by choosing an appropriate angle α of the pump beams for required THz-frequency. The angle α is formulated from geometric relation of A, B and C, $A^2C^2=B^2C^2=A^2B^2$, as shown in Fig. 1(c).

$$\alpha = 2 \arccos \left(\sqrt{\frac{-(k_1 + k_2)^2 + \frac{16\pi^2}{(\lambda_{\text{THz}}/n_{\text{THz}})^2}}{4(k_1 - k_2)^2 - (k_1 + k_2)^2}} \right) \quad (2)$$

Generated THz-wave can propagate without influence of phase mismatching in the direction of propagating direction, just like as surf rider on nonlinear polarization waves, as shown in Fig. 1(b). The required angle for frequency tuning was shown in Fig. 2(a) internal and (b) external crystal. Phase matching condition is satisfied by changing the angle α for required THz-wave and pumping wave wavelength. And slightly narrow tunability (about 300 GHz at around 3 THz generation) is obtained at a fixed angle, $\alpha=4.0$ degrees.

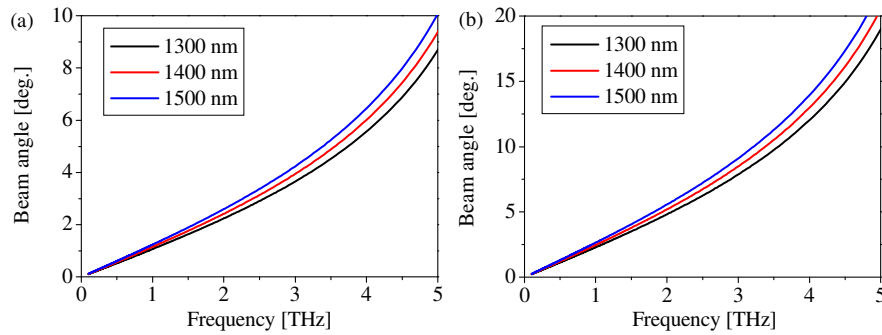


Fig. 2. Tuning angle (a) internal and (b) external of crystal under 1300, 1400 and 1500 nm of pumping wavelength of λ_1 .

3. Experimental setup

Figure 3 shows the schematic of experimental setup. A pump source for DFG process was same as our previous works [20], and which has a tunable range of 1250 to 1500 nm, 15 ns of pulse duration and 0.88 mJ of pulse energy. An output of the source with dual wavelength was focused by circular lens ($f=500$ mm) before divided by half beam splitter, and combined again with finite angle. The spot diameter of the combined beam was 0.45 mm. The 5 mol % MgO-doped lithium niobate crystal ($\text{MgO}:\text{LiNbO}_3$) used in the experiment was cut from a $5 \times 65 \times 6$ mm wafer, and the x-surfaces at both ends were mirror-polished. An array of seven Si prism couplers was placed on the y-surface of the $\text{MgO}:\text{LiNbO}_3$ crystal. The y-surface was also mirror-polished to minimize the coupling gap between the prism base and the crystal surface, and to prevent scattering of the pump beam, which excites a free carrier at the Si prism base. The polarizations of the pump and THz waves were both parallel to the Z-axis of the crystals. The THz-wave output was measured with a fixed 4 K Si bolometer.

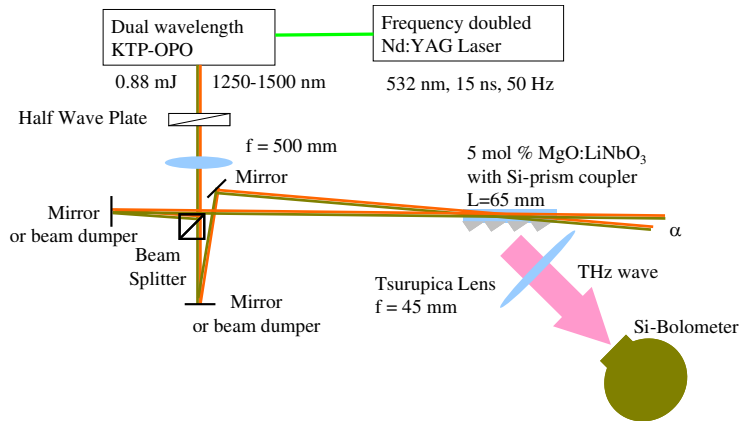


Fig. 3. Schematic of experimental setup for Cherenkov phase matching THz-wave generation with surfing configuration.

4. Results and discussion

Input-output properties of THz-wave for pumping energy are shown in Fig. 4 at 1.0 THz generation with $\alpha=2.49$ degrees. Circles and triangles denotes THz-wave output signal with combined beams and with single beam by dumping the other beam before entrance to the crystal, respectively. Maximum pumping energy of only 0.44 mJ was achieved at single beam pumping, because a half of whole pumping energy was dumped as shown in Fig. 3. The vertical axis is the THz-wave pulse energy calculated from the output voltage of a Si-bolometer detector, a pulse energy of about 101 pJ/pulse corresponded to a Si-bolometer voltage output of 1 V when the repetition rate was less than 200 Hz. As shown in the figure, remarkable enhancement of THz-wave generation with surfing configuration, whose magnetic was about 50 times, was successfully observed. Inset of Fig. 4 shows double logarithmic plot of input-output properties. Slope efficiency under combined beams and single beam pumping were almost same values. It means that enhancement factor of about 50 was a result of a suppression of phase miss-matching.

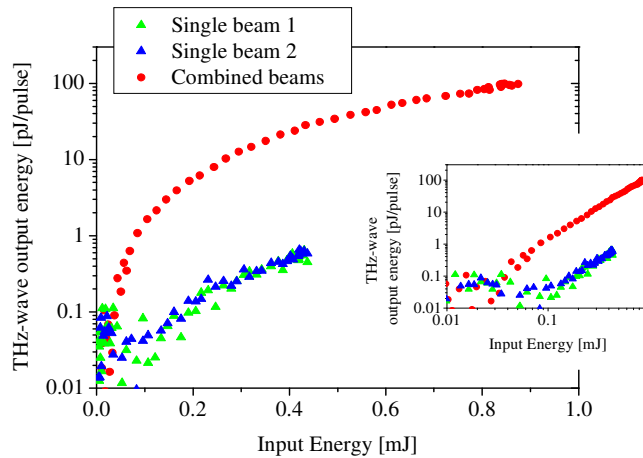


Fig. 4. Input-output property of THz-wave for pumping energy at 1.0 THz generation with $\alpha=2.49$ degrees. Circles and triangles denotes THz-wave output signal with combined beams and with single beam. Inset shows double logarithmic plot of input-output properties.

The generated THz-waves at different position in the crystal were in-phase each other, and outputted THz-wave was enhanced. Intensity of overlapping in-phase THz-waves in an absorptive media was calculated as shown in Fig. 5. A 5 mol % MgO-doped Lithium Niobate crystal at THz-wave frequency region would have about 30 cm^{-1} of absorption coefficient [21]. The enhancement effect of in-phase interference would be effective for about 2 mm of traveling distance of THz-wave, this fact leads optimum pumping beam width in y-axis direction is about 1.8 mm. In this study, pumping beam width in y-axis was about 0.45 mm, results in a propagating length of a THz-wave was about 1.2 mm. Higher enhancement above 50 would be obtained with tight focused beam only for z-axis by cylindrical lens.

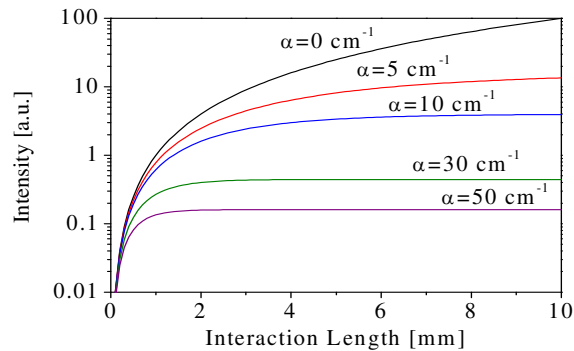


Fig. 5. Calculated intensity of overlapping in-phase THz-waves in an absorptive media.

Figure 6 shows THz-wave output characteristics under fixed pumping wavelength of 1300 nm and several fixed angle, 2.49, 3.80 and 5.03 degrees. Maximum THz-wave output at each angle was obtained at higher frequency in the bigger angle, α . Obtained peaks of THz-wave output were about 1.1, 1.6 and 1.9 THz, respectively. The relation between the angle and the frequency where maximum output was obtained agree well with Eq. (2), 1.08, 1.61 and 2.07 THz under 1300 nm pumping respectively. Tuning range for higher frequency region was remarkably improved compare with our previous collinear and not tight focused configuration. THz-wave output at around 4 THz was successfully obtained.

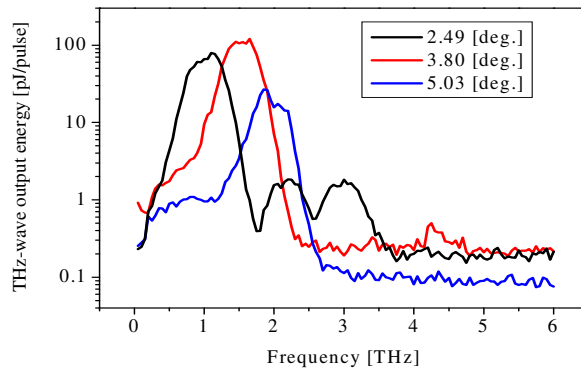


Fig. 6. THz-wave output spectra under fixed pumping wavelength of 1300 nm and several fixed angle, 2.49, 3.80 and 5.03 degrees.

As described in our previous work [22], because the linewidth of each pumping wave is about 60 GHz, the source linewidth is about 100 GHz, which is slightly broader than that obtained from sources such as injection-seeded terahertz parametric generator [23] or DAST crystal-based difference-frequency generators [24]. This occurs because the linewidth of the THz-wave depends on that of the pumping source.

The spectrum with $\alpha=2.49$ degrees pumping had two dips at 1.8 and 2.6 THz. It caused by perfect phase miss-matching of THz-wave propagation. Figure 7 shows calculated nonlinear polarization distributions at (a) 1.8 and (b) 2.6 THz generation with $\alpha=2.49$. THz-wavelength in the crystal at 1.8 THz generation is $32.2 \mu\text{m}$. Generated THz-wave at point “a” in Fig. 7 interferes with that at point “b”, which has a phase difference by π compare to that of point “a”, results in destructive interference. Similarly, and adding higher order interference, generated THz-wave at point “c” has destructive interference with that at point “d”. THz-wave generation was observed at around the dips, because perfect phase miss-matching was relaxed at these frequencies. We have not yet completed the analytical solution predicting the frequency due to destructive interference, and it remains an area of future work.

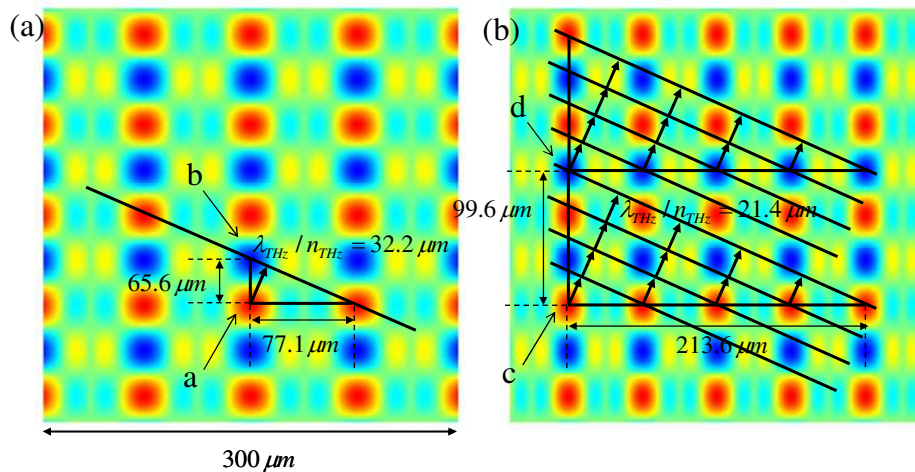


Fig. 7. Calculated nonlinear polarization distributions at (a) 1.8 and (b) 2.6 THz generation with $\alpha=2.49$.

Broader tuning range would be obtained by controlling the angle α within about only 2.5 degrees range. Because lithium niobate is strongly absorbing at THz-frequencies, the beam-crossing position was set near the crystal surface to generate the THz-wave. In this configuration, the pumping beam passing through a Si prism yields an optical carrier excitation in Si that prevents THz-wave transmission, while the interaction length decreases at larger pumping angles, α . The interaction lengths, $l = 2D / \tan \alpha$, where D is the beam diameter, are 21.4 and 10.7 mm for α s of 2.49° and 5.03° , respectively. If we use a shorter lithium niobate crystal, the optical carrier excitation can be avoided, and larger pumping angles can be employed to obtain higher-frequency generation.

5. Summary

In conclusion, we proposed and demonstrated Cherenkov phase matching with surfing configuration for bulk crystal. We successfully obtained efficient THz-wave generation for about 4 THz wave region, and the enhancement factor was about 50. The method is very simple way to obtain higher frequency and efficient generation of THz-wave, because the method does not require a special device such as slab waveguide structure.

Acknowledgments

The authors thank Dr. C. Otani and K. Maki of RIKEN, Japan, for their help of using a Si-bolometer. The authors thank C. Takyu for his excellent work coating the crystal surface, and T. Shoji for polishing the crystals superbly. This work was supported in part by the National Institute of Communications Technology, Japan.